AIP | Review of Scientific Instruments

Impedance spectroscopy using maximum length sequences: Application to single cell analysis

Shady Gawad, Tao Sun, Nicolas G. Green, and Hywel Morgan

Citation: Review of Scientific Instruments **78**, 054301 (2007); doi: 10.1063/1.2737751
View online: http://dx.doi.org/10.1063/1.2737751
View Table of Contents: http://scitation.aip.org/content/aip/journal/rsi/78/5?ver=pdfcov
Published by the AIP Publishing

Impedance spectroscopy using maximum length sequences: Application to single cell analysis

Shady Gawad,[a] Tao Sun, Nicolas G. Green, and Hywel Morgan[b]
Nanoscale Systems Integration Group, School of Electronics and Computer Science, University of Southampton, SO17 1BJ United Kingdom

(Received 21 February 2007; accepted 16 April 2007; published online 29 May 2007)

A maximum length sequence (MLS) is used to perform broadband impedance spectroscopy on a dielectric sample. The method has a number of advantages over other pulse-based or frequency sweep techniques. It requires the application of a very short sequence of voltage steps in the microsecond range and therefore allows the measurement of time-dependent impedance of a sample with high temporal resolution over a large bandwidth. The technique is demonstrated using a time-invariant passive *RC* network. The impedance of single biological cell flowing in a microfluidic channel is also measured, showing that MLS is an ideal method for high speed impedance analysis. © *2007 American Institute of Physics.* [DOI: 10.1063/1.2737751]

I. INTRODUCTION

The maximum length sequence (MLS) measurement technique is widely used in the field of acoustics for measuring concert hall acoustics[1] as well as loud-speaker transfer functions.[2] A number of other techniques are also employed in acoustic testing, such as frequency sweeps, chirps, or pulse-based methods. Each of these methods has merits and drawbacks, depending on the specific application.[3]

The MLS method is based on a cross correlation between the input and output signals to obtain the periodic impulse response (PIR) of the system being measured. The cross-correlation algorithms employed are efficient in noise rejection and the technique can be compared to quadrature demodulation in the frequency domain.[4] MLS has been proposed as a general technique for measuring the transfer function of any linear system.[4] Therefore, the technique is applicable to the analysis of the electrical impedance of any arbitrary network in particular. Although most of the research work and publications on MLS and other pseudorandom noise sources are found in the acoustic field, the technique is being gradually adopted by researchers for diverse applications. For example, Weckström *et al.*[5] injected a white-noise-modulated current into cells for the determination of cellular input impedance of nonspiking neurons. Schneider[6] in 1996 proposed the idea of using MLS in a multifrequency electrical impedance tomography (EIT) system for the observation of long bone fracture healing and the characterization of electrical bioimpedance. Rufer *et al.*[7] used MLS for characterizing microelectromechanical system (MEMS) structures to determine mechanical and thermal behavior. More recently the MLS technique was used in a laser Doppler vibrometer-based acoustic land mine detection technique as an acoustic excitation signal[8,9] and to sonar systems for ocean fisheries and zooplankton survey.[10] Amrani *et al.*[11] used a pseudorandom binary sequence for application in gas sensing.

Compared to a single pulse of the same amplitude, much more energy is fed into the system under test, which results in an increased signal-to-noise ratio (SNR). This is because the excitation signal is distributed over the whole measurement period. The crest factor (the ratio between the signal peak and rms) is only 1 for MLS, whereas a chirp signal has a crest factor of $\sqrt{2}$. For impedance spectroscopy of biological systems, a low crest factor is desirable because this limits the applied current peaks, preventing electrode damage due to electrochemical processes or unnecessary stress applied to the sample.

II. IMPEDANCE SPECTROSCOPY

Impedance spectroscopy is a nondestructive label-free analytical tool which has found widespread use in many scientific and technological areas, including the monitoring and analysis of corrosion,[12,13] batteries,[14] fuel cells,[15] semiconductors,[16,17] electrochemical kinetics/mechanisms,[18–21] and biological and biomedical systems.[22–24] In all these examples the static or dynamic complex impedance spectrum $\tilde{Z}(j\omega)$ of a device, network, or sample contains information on the physicochemical properties. In particular, impedance (or dielectric) spectroscopy has been used to measure the passive electrical properties of biological cells for many years.[25–28]

The complex electrical impedance of a system $\tilde{Z}(j\omega)$ is calculated from the measured current $I_r(t)$ passing through the system when a spectrally dense voltage source $U_s(t)$ is applied to the sample.

[a]Present address: LMIS4-STI-EPFL, Swiss Federal Institute of Technology, 1015 Lausanne, Switzerland; electronic mail: shady.gawad@gmail.com
[b]Electronic mail: hm@ecs.soton.ac.uk

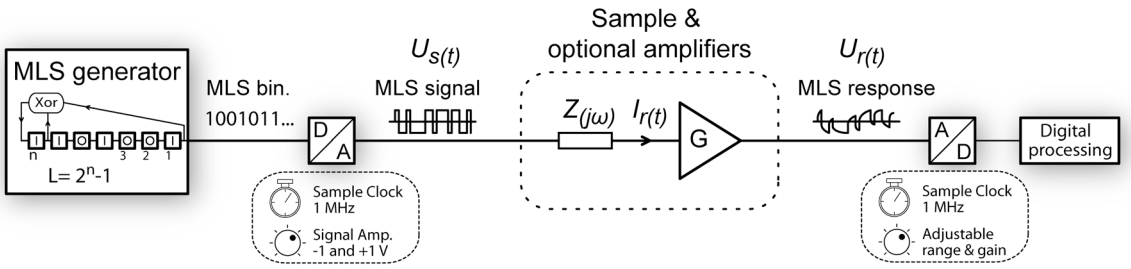

FIG. 1. Diagram showing the MLS measurement technique. The MLS is generated in software, converted to an analog voltage with a D/A converter, and then applied to the sample. An optional transimpedance amplifier converts the current response to a voltage. The signal is converted to digital with an A/D converter. The digital data stream is then processed with minimal delay by a standard desktop computer.

$$\tilde{Z}(j\omega) = Z_{\mathrm{Re}}(\omega) + jZ_{\mathrm{Im}}(\omega) = \frac{U(j\omega)}{I(j\omega)} = \frac{\mathcal{F}\{U_s(t)\}}{\mathcal{F}\{I_r(t)\}}$$

$$= \frac{\phi_0}{\mathcal{F}\{I_r(t)\}}, \tag{1}$$

where $j^2=-1$ is the imaginary unit and ω (rad/s) is the angular frequency.

For an MLS the applied voltage signal $U_s(t)$ has a quasiflat spectral power ϕ_0 over the bandwidth of interest. It is thus possible to recover the complex impedance spectrum using a single time-to-frequency domain transformation, i.e., the Fourier transform $\mathcal{F}\{X(t)\}$, on the recovered system response signal $I_r(t)$. Generally since most analog-to-digital converters (ADC) have a voltage input, a transimpedance amplifier is used to convert the current response $I_r(t)$ into a voltage signal $U_r(t)$ with a suitable dynamic range (Fig. 1).[29]

The transimpedance amplifier has the disadvantage that it will influence the transfer function of the system and will in general require a calibration procedure. An alternative passive method involves measuring the voltage dropped across a fixed value resistor, but this is prone to noise and is unsuitable for measuring low currents.

III. MAXIMUM LENGTH SEQUENCE (MLS)

A. Principle

Developments in the field of Lab on a Chip have made impedance analysis of single micron-sized objects such as cells and beads possible. In particular, we and others[30–34] have developed methods in performing impedance spectroscopy of single cells at high speed. In this technique, a number of superimposed rf sine signals are used to measure the impedance of single cells flowing through a microchannel. Impedance measurements based on multiple frequency measurements can be used to characterize cellular properties, such as size, membrane capacitance, etc. and to distinguish differences in cell subpopulations.[35,36] However, there is a need to perform multifrequency analysis in a short time window. Frequency sweep methods are unsuitable because the typical transit time of a cell is of the order of a millisecond. Multiple superimposed frequency excitations require one dedicated rf lock-in demodulator for each frequency, which is clearly impractical. Therefore, one approach is to use a spectrally dense signal such as chirp or MLS (Fig. 2).

The MLS technique is particularly attractive because of the high computational efficiency of processing and a good signal-to-noise ratio. The use of MLS in measuring the impulse response of a linear time invariant (LTI) system has been established for many years and can be traced back to 1960.[37,38] One of the advantages of the MLS technique is that the energy is delivered to the system regularly in time, because the power spectrum of the excitation signal has a homogeneous frequency distribution; it has a quasiflat spectrum (white noise like) expect for dc.[39]

In biological impedance measurements the electrode-electrolyte interface presents a number of problems. The interfacial impedance, which is generally capacitive, is in series with the sample and may thus hinder measurements at low frequencies because the interface impedance can be orders of magnitude larger than that of the cell suspension. It is also preferable to use a low excitation voltage to reduce any

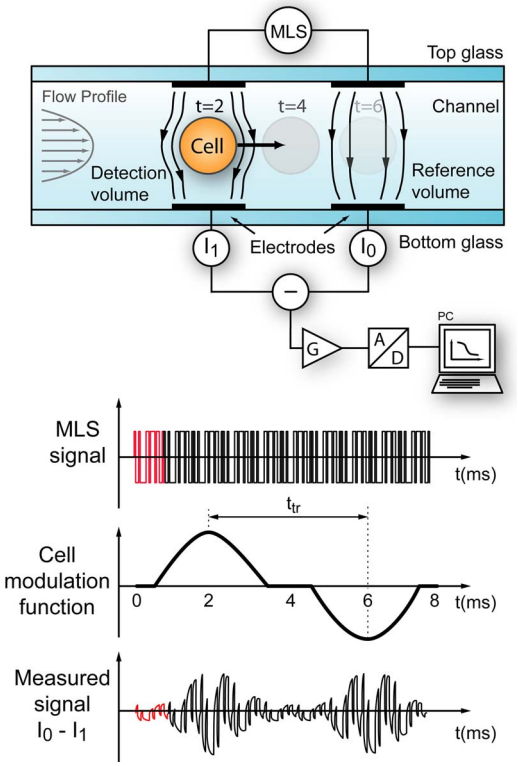

FIG. 2. Principle of using MLS to measure the complex impedance change due when biological cells pass through a capillary channel. The signal amplification electronics contains a current to voltage conversion stage and a differential amplifier, gain $G=150$. The MLS signal is sent continuously to the sensing electrodes, the passage of a cell imbalances the sensor and the differential current is recorded and processed using a computer.

electrochemical process which could potentially damage the electrodes or cause nonlinearities in the measurements.[40] The voltages used for impedance measurement are generally much lower than those used in techniques such as dielectrophoresis[41–43] and are thus less likely to cause any damage to the cells being investigated. In the megahertz range, excitation signals up to 1 V can be safely used with standard phosphate buffered solution (PBS). The MLS method has advantages in that applied voltage is constant and can be set to within the linear regime for the electrodes as well as safe for the cells.

B. Generation of MLS

In this section we describe the generation of the MLS.[4,44,45] Algorithms for generating the MLS and retrieving the system impulse response have been developed by several authors.[38,39,46,47] The MLS is a pseudorandom binary sequence (PRBS) composed of a sequence of 1 and 0, generated recursively using a series of digital shift registers with selected XOR feedback, called taps (Fig. 1). The length L of the MLS given by $L=2^n-1$ with n denoting the order of the sequence and also the number of digital shift registers. The feedback loop is recursively implemented as follows:

$$a_n = \left(\sum_{i=1}^{n} c_i a_i \right) \mathrm{mod}(2). \tag{2}$$

In Fig. 1, the output digital signal comes from register a_1 and the new generated digital signal goes to register a_n, which depends on the states of all the registers and the corresponding feedback coefficients c_i. Note that the index i runs from 1 to n along the shift register from right to left.

The primitive polynomial of the sequence is defined from the feedback coefficients c_k,

$$f(x) = 1 + \sum_{k=1}^{n} c_k x^k. \tag{3}$$

In this equation the index k runs from 1 to n along the shift register from left to right.

With any given initial state of the shift registers (except all zeros) an MLS can be generated. A "characteristic" MLS, also called self-similar, can be generated by selecting appropriate initial states for the shift register values.[48] In practice, the 1 and 0 logical states are often mapped into a negative level and positive level, respectively, to produce a sequence for which the net sum is close to zero.

C. Signal processing

The most important property of any MLS is that, expect for a small dc error, its periodic autocorrelation function $\phi_{nn}(l)$ is the two valued Kronecker function $\delta(l)$,[39]

$$\phi_{nn}(l) = \frac{L+1}{L}\delta(l) - \frac{1}{L}, \tag{4}$$

with

$$\delta(l) = \begin{cases} 1, & \text{for } l = 0 \\ 0, & \text{for } l \neq 0, \end{cases} \tag{5}$$

where l is calculated modulo L. A longer MLS sequence produces a smaller error in the autocorrelation function, since the second term of Eq. (4) representing the dc error will be smaller. The influence of this error also depends on the physical properties of the measured sample, and whether it is dc coupled or not to the measurement circuitry. One way to correct for the dc error is to use a so called perfect periodic autocorrelation signal which can be obtained by selecting appropriate values for the MLS signal instead of +1 and −1,[49]

$$V_{\text{positive}} = 1,$$

$$V_{\text{negative}} = \frac{-1}{1 + 2/\sqrt{L+1}}. \tag{6}$$

The discrete impulse response $g(l)$ of an LTI system under test can be retrieved from the cross-correlation function between the input and output signals $\phi_{ny}(l)$ and the autocorrelation function $\phi_{nn}(l)$ of the input signal.

$$\phi_{ny}(l) = g(l) * \phi_{nn}(l) \cong g(l) * \delta(l) = g(l), \tag{7}$$

where the $*$ operator denotes the periodic discrete linear convolution. Since convolving any function with the Kronecker delta function equates to the function itself, a direct relationship between the impulse response of the system and the cross-correlation function $\phi_{ny}(l)$ is implied.

Cohn and Lempel[47] demonstrated that the periodic cross-correlation function can be effectively done using a fast M transform (FMT) which comprises two permutations and a fast Hadamard transform (FHT). Borish and Angell[44] showed that this computation requires only $2.5n \log_2(n)$ addition operations. In this work, the algorithm was implemented in C (as a mex file in MATLAB). The algorithm structure is outlined in Fig. 3.

Additional improvements to the SNR are also proposed by these authors. Specifically because the desired signals add coherently while the noise adds incoherently, they suggested preaveraging a number m of response sequences, which gives an improvement in the SNR of $\sqrt{m}$.[44] Using this noise reduction technique implies that rapid changes in the system impedance are averaged out, which results in a trade off between noise reduction and the ability to measure dynamic changes in time. It is also important to note that the response obtained with this technique is the PIR, which only reduces to the impulse response (IR) if the system relaxation time is shorter than the generation time of the MLS used.

A fast Fourier transform (FFT) is then used to convert each impulse response to the corresponding transfer function of the system using FFTW.[50] The transfer function is used to obtain the impedance of the system. The impulse response is padded with an extra zero in order to obtain an impulse length of 2^n before the FFT. The FFT calculation returns a complex value spectrum with 2^{n-1} frequency points. The highest measured frequency $f_{\max}$ is given by the Nyquist-Shannon sampling theorem as half of the sampling rate f_s. The frequency resolution is defined as the difference between

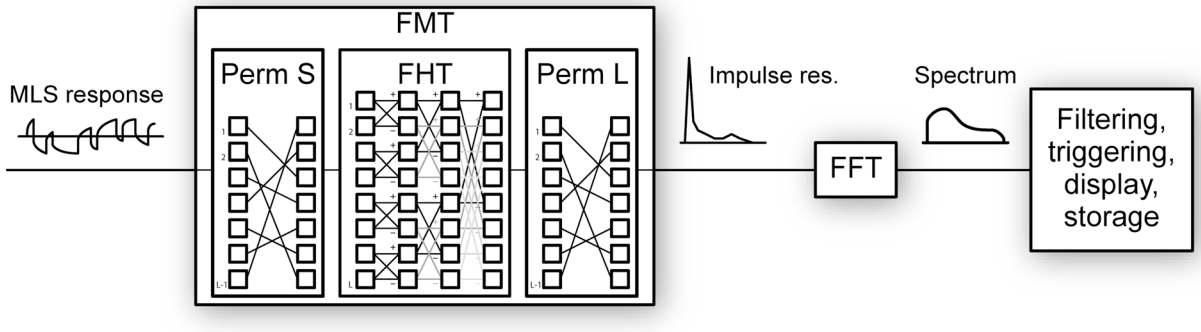

FIG. 3. The digitized MLS response signal is processed using two permutation matrices (S and L) and a fast Hadamard transform (FHT) to recover the periodic impulse response. A complex fast Fourier transform (FFT) is then used to obtain the complex impedance spectrum of the system.

two adjacent measured discrete frequencies. Since the discrete frequency points are evenly spaced the minimum frequency $f_{\min}$ also corresponds to the frequency resolution f_{res},

$$f_{\max} = f_s/2, \tag{8}$$

$$f_{\min} = f_{\text{res}} = f_s/2^n. \tag{9}$$

IV. EXPERIMENT

A. Hardware and implementation

The recent availability of fast processors and analog-to-digital (A/D) converters has allowed the MLS technique to be implemented for real-time broadband impedance spectroscopy. At the time of writing A/D converters with sample rates of 200 megasamples/s and precisions in the order of 12–16 bits are commercially available. The MLS, in binary form, is generated using software written in MATLAB and then converted to a voltage step sequence of fixed amplitude and timing using a digital-to-analog (D/A) converter (NI-6251, National Instruments, USA). The MLS response from the device is digitized using an A/D converter on the same board. Both D/A and A/D tasks are started simultaneously with a synchronous clock for the conversions. The hardware has to minimize clock-induced time jittering as this could add a significant white noise source to the recovered spectrum.[2]

In the present case the sequence has a length of 1023 samples (order $n=10$) and is generated using a sample rate of 1 MHz, i.e., approximately 1000 times per second. The 1 MHz clock frequency is limited by the data acquisition hardware, and the length of the sequence was a compromise between resolution and the sequence period (approximately 1 ms). For an MLS of order 10, a sampling rate at 1 MHz, and according to Eqs. (8) and (9), the spectrum lies between 976.5625 Hz and 500 kHz. The software performs a number of post processing operations, including optional time filters, event triggering, data plotting, and storage.

B. Test systems

Two test systems were used to evaluate the MLS method. The first is an *RC* network, where the measured results are compared with a model of the system and the MLS sequence. The second test was the measurement of erythrocytes (red blood cells) flowing in a microfabricated microfluidic impedance sensing chip.

1. RC network

The network shown in Fig. 4 was used to test the MLS system and to validate the behavior against known parameters. Measurement was performed without current to voltage conversion, and the input impedance of the data acquisition board was used as the sensing resistor and is therefore included in the modeling.

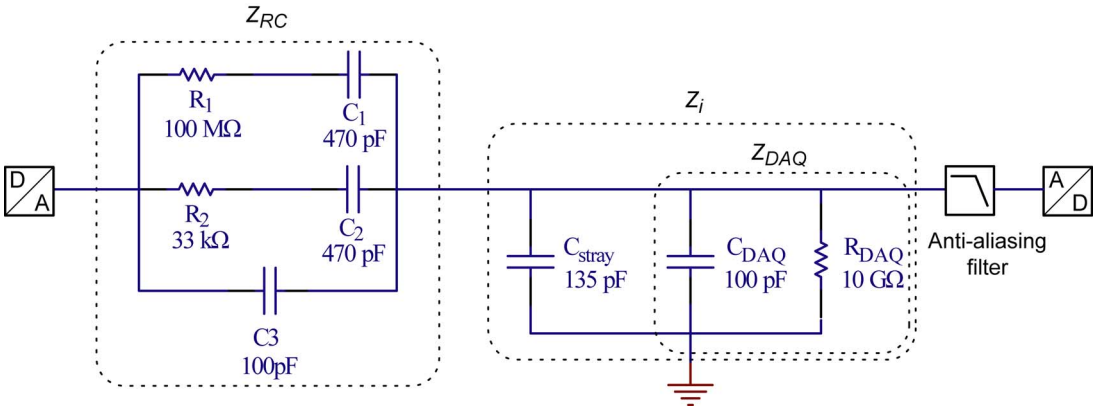

FIG. 4. Schematic of the *RC* network used to test the MLS system, showing the test network Z_{RC}, the input impedance of the acquisition system Z_{DAQ}, and the stray capacitance C_{stray}.

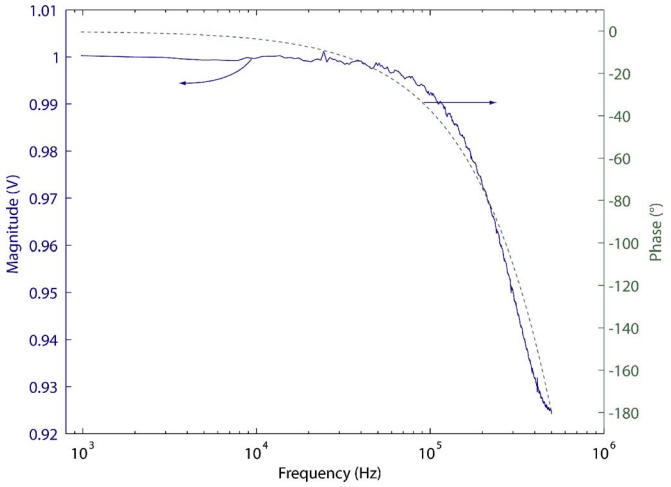

FIG. 5. The transfer function of the data acquisition board, measured by connecting the input and output with a coaxial cable, showing the influence of the antialias filter and the phase delay at higher frequencies.

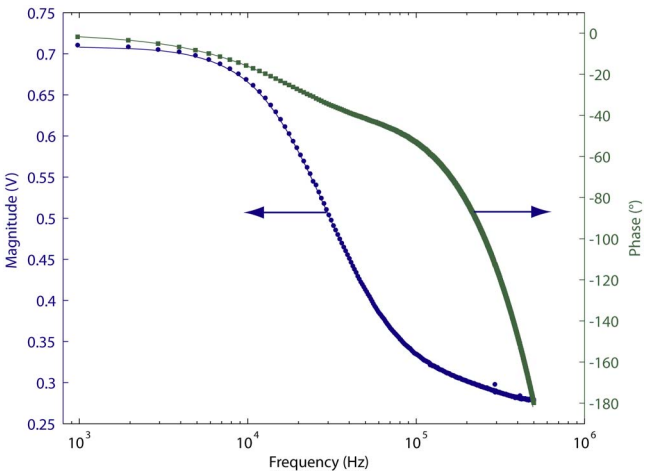

FIG. 6. Plot of the magnitude and phase of the transfer function of the network. The model is shown as a solid line and includes the low pass filter. The experimentally measured transfer-function data is plotted as symbols.

Because no transimpedance stage is used, the input impedance of the A/D acquisition board Z_{DAQ} influences the recovered spectrum, as does the A/D antialiasing low pass filters (specified with −3 dB at 1.7 MHz). The transfer function H_{sys} of the RC network measured with the A/D acquisition board is defined as

$$H_{\mathrm{sys}} = \frac{Z_i}{Z_i + Z_{RC}}, \tag{10}$$

with

$$Z_i = \frac{Z_{\mathrm{DAQ}}}{1 + j\omega Z_{\mathrm{DAQ}} C_{\mathrm{stray}}} = \frac{R_{\mathrm{DAQ}}}{1 + j\omega R_{\mathrm{DAQ}}(C_{\mathrm{DAQ}} + C_{\mathrm{stray}})}, \tag{11}$$

where Z_i comprises the input impedance Z_{DAQ} of the data acquisition board (NI 6251 DAQ) and the stray capacitance C_{stray} of the coaxial cable. The values for the input impedance (taken from the datasheet) are 10 GΩ resistor (R_{DAQ}) in parallel with a 100 pF capacitor (C_{DAQ}), see Fig. 4.

After some algebraic treatment, the impedance Z_{RC} of the RC network is

$$Z_{RC} = \frac{A_1(j\omega)^2 + A_2(j\omega) + 1}{A_3(j\omega)^3 + A_4(j\omega)^2 + A_5(j\omega)}. \tag{12}$$

The coefficients A_i (i=1–5) are given in the appendix.

The transfer function of the low pass antialias filter H_F was determined by directly connecting the analog output (D/A) to the input (A/D) with a coaxial cable. Figure 5 show the measured transfer function spectrum for a 1 V excitation signal. The phase was found to increase to 180° at high frequency; this corresponds to a delay of one clock cycle in the impulse response. Since both the D/A and the A/D convert samples simultaneously the impulse peak will not be measured on the first clock but only on the second clock due to nonperfect slew rates and such of the acquisition board amplifiers. This delay and resulting phase error can be easily compensated in software.

The magnitude and phase of the transfer function of the RC network system including the filter $H_{\mathrm{sys\_}F}$ are given by

$$|H_{\mathrm{sys\_}F}| = |H_{\mathrm{sys}}| \times |H_F|, \tag{13}$$

$$\angle H_{\mathrm{sys\_}F} = \angle H_{\mathrm{sys}} + \angle H_F, \tag{14}$$

The MLS sequence is generated from the shift register using recursive steps. The output MLS signal, with +1 and −1 levels, is expressed as a time dependent function by the superposition of unit step functions $U_0(t)$,

$$X_{\mathrm{MLS}}(t) = U_0(t) + 2\sum_{i=1}^{m} (-1)^i U_0(t - t_i), \tag{15}$$

where the index i indicates the successive changes in the MLS signal polarity and t_i is the time when each corresponding signal step occurs.

The output response of the system $Y_{\mathrm{sys}}(s)$ to an MLS excitation $X_{\mathrm{MLS}}(s)$ can be expressed in the s domain as:

$$Y_{\mathrm{sys}}(s) = X_{\mathrm{MLS}}(s) H_{\mathrm{sys}}(s). \tag{16}$$

According to the time shift property of the Laplace transform and the superposition principle, the inverse Laplace transform of Eq. (16) is

$$Y_{\mathrm{sys}}(t) = \left[Y_{\mathrm{sys0}}(t) + 2\sum_{i=1}^{m} (-1)^i Y_{\mathrm{sys0}}(t - t_i) U_0(t - t_i) \right], \tag{17}$$

which is the output response of the system in the continuous time domain corresponding to the MLS excitation. In this equation, $Y_{\mathrm{sys0}}(t) = k_1 e^{s_1 t} + k_2 e^{s_2 t} + k_3 e^{s_3 t}$ is the response of the system to a single unit step excitation signal $U_0(t)$ in the time domain.

The same data processing algorithms including the FMT and FFT are applied to the simulated data to retrieve the system transfer function.

Figure 6 shows that the data are in excellent agreement (within 1%) of the model, indicating that the MLS measurement technique can be used to characterize the transfer function of a passive RC network.

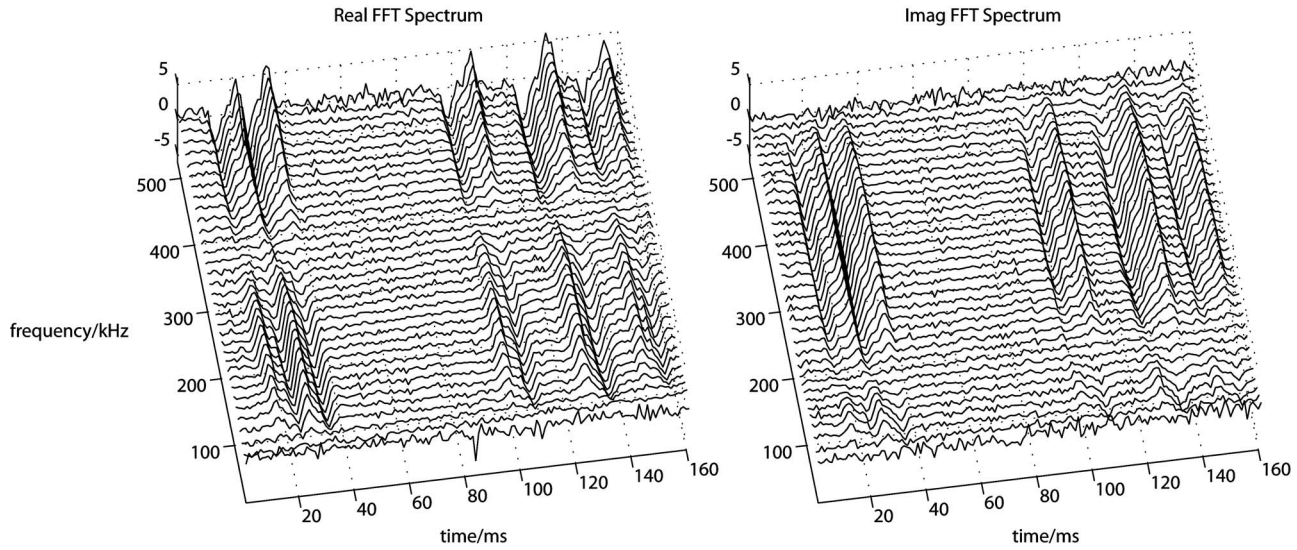

FIG. 7. Moving averaged spectrogram showing five consecutive red blood cell events as measured using a differential capillary impedance sensor. Although a 512-frequency-point spectrogram is obtained only a subset of the data is presented here for clarity.

2. Single cell impedance measurement

The sensor chip for single cell impedance analysis is described elsewhere[32] and is shown in Fig. 2. It consists of a capillary channel, $40\times 20\ \mu m^2$ cross section with two pairs of electrodes placed on opposite sides of the channel. The impedance is measured using a transimpedance amplifier followed by a differential amplification stage with gain $G=150$. Because the cells continuously flow between the electrodes, the system cannot be considered time invariant.

Erythrocytes were harvested from healthy donors and suspended in a PBS (conductivity of $1.6\ S\ m^{-1}$) prior to flowing through the microfluidic channel using a pressure driven flow. In the cell measurements, the impedance is measured differentially and is time varying. The change in impedance due to a cell is only between 1% and 5% of the total channel impedance.[33] The slow (long time period) variations in impedance due to external parameters were filtered using a moving average offset compensation.

The time averaged spectrogram is therefore flat in the absence of a cell. The MLS data for single cells flowing through the device consists of a spectrogram as shown in Fig. 7. Each cell generates two successive impedance spectral pulses (one positive and one negative) as it passes over each part of the differential sensor (see Fig. 2). The data show that the spectrum of single cells passing through the detection area in a 20 ms time frame can be clearly resolved (up to the frequency limit of the acquisition system) using a MLS having a generation time of a millisecond.

V. DISCUSSION

The measurement of the *RC* circuit indicates that the MLS technique can be used to measure the transfer function and therefore the impedance of a (linear time invariant) network. Preliminary data also show that the technique can also be used to detect the movement of cells through the microchip and to measure the low frequency part of the transfer function, up to 500 kHz. In this frequency range, the measurement of the cell is limited by the presence of the electrode-electrolyte interface capacitance (the double layer). The data show for the first time that single cell events can be measured across a wide band of frequencies; only measurements at two or three simultaneous frequencies have been reported previously.[36] The method allows real-time spectrograms of the transfer function (and by implication the complex impedance) of cells passing through a microfluidic system.

The data show that although the cell measurement system is not time invariant, this could be less problematic than is usually the case in acoustic measurements. The results indicate that the MLS measurement technique shows promise for high speed single cell analysis. The flexibility of the system means that the signals can be modified in real time to compensate for various deleterious effects such as parasitic elements or the electrode-electrolyte impedance. These elements can be compensated for using techniques borrowed from acoustics, such as filters which proportionally increases the voltage of the low frequency components of the sequence. The precompensated signal would increase the smaller measured current signal at low frequencies to compensate for the interfacial capacitance. Because the system impedance is measured at a high rate, it would be possible to implement a fast-feedback compensation loop which could take into account slow variations in the impedance due to external effects such as temperature changes or changes in flow speed or conductivity.

In this article we have shown that the MLS technique can measure the transfer function of an electrical system and is able to perform fast broadband dielectric spectroscopy. The underlying theory of MLS generation and processing has been presented and a system has been described which can measure the transfer function of an *RC* network. The measured response is in excellent agreement with an analytical model. The MLS technique is relatively easy to implement and can be used to measure the spectrum of a biological system with a rate and resolution not reported previously. Future work will concentrate on extending the frequency

bandwidth and developing applications to measurement of rapid dynamic changes in biological cellular systems following electrical or chemical stimuli.

ACKNOWLEDGMENTS

One of the authors (S.G.) would like to acknowledge the funding from the SNSF fellowship. He also would like to thank Professor Ph. Renaud for his support in many aspects of this work. The work is partly supported by the funding from Life Science Initiative, University of Southampton. Finally one of the authors (S.G.) would like to gratefully acknowledge Professor P. Gascoyne, Professor B. Persson, and B. Böhmer for the discussions and suggestions.

APPENDIX

The coefficients A_i $(i=1-5)$ in Eq. (12) are given by

$$A_1 = R_1R_2C_1C_2, \quad A_2 = R_1C_1 + R_2C_2,$$

$$A_3 = R_1R_2C_1C_2C_3,$$

$$A_4 = R_1C_1(C_2 + C_3) + R_2C_2(C_1 + C_3),$$

$$A_5 = C_1 + C_2 + C_3.$$

[1] Y. Ando, *Concert Hall Acoustics* (Springer, New York, 1985).
[2] J. Vanderkooy, J. Audio Eng. Soc. **42**, 219 (1994).
[3] D. Griesinger, 101st Convention of the Audio Engineering Society, Los Angeles Convention Center (1996) http://www.aes.org/publications/preprints/search.cfm.
[4] D. D. Rife and J. Vanderkooy, J. Audio Eng. Soc. **37**, 419 (1989).
[5] M. Weckstrom, E. Kouvalainen, and M. Juusola, Pfluegers Arch. **421**, 469 (1992).
[6] I. Schneider, Engineering in Medicine and Biology Society, 1996, Bridging Disciplines for Biomedicine, Proceedings of the 18th Annual International Conference of the IEEE, October 31–November 3, 1996, Vol. 5, pp. 1934–1935.
[7] L. Rufer, S. Mir, E. Simeu, and C. Domingues, Journal of Electronic Testing-Theory and Applications **21**, 233 (2005) (online).
[8] N. Xiang and J. M. Sabatier, Proc. SPIE **3720**, 390 (1999).
[9] N. Xiang and J. M. Sabatier, IEEE Trans. Geosci. Remote Sens. **1**, 292 (2004).
[10] N. Xiang and D. Chu, Proceedings of the ICSP'04, 7th International Conference on Signal Processing, August 31-September 4, 20042004 Vol. 3, pp. 2433–2436.
[11] M. E. H. Amrani, R. M. Dowdeswell, P. A. Payne, and K. C. Persaud, Sens. Actuators B **47**, 118 (1998).
[12] F. Mansfeld, J. Appl. Electrochem. **25**, 187 (1995).
[13] P. L. Bonora, F. Deflorian, and L. Fedrizzi, Electrochim. Acta **41**, 1073 (1996).
[14] H. Arai, S. Muller, and O. Haas, J. Electrochem. Soc. **147**, 3584 (2000).
[15] B. Andreaus, A. J. McEvoy, and G. G. Scherer, Electrochim. Acta **47**, 2223 (2002).
[16] P. R. Bueno, S. A. Pianaro, E. C. Pereira, L. O. S. Bulhoes, E. Longo, and J. A. Varela, J. Appl. Phys. **84**, 3700 (1998).
[17] R. A. Kumar, M. S. Suresh, and J. Nagaraju, IEEE Trans. Electron Devices **48**, 2177 (2001).
[18] C. Gabrielli, M. Keddam, N. Portail, P. Rousseau, H. Takenouti, and V. Vivier, J. Phys. Chem. B **110**, 20478 (2006).
[19] C. Gabrielli and M. Keddam, Electrochim. Acta **41**, 957 (1996).
[20] A. Kisza, J. Thonstad, and T. Eidet, J. Electrochem. Soc. **143**, 1840 (1996).
[21] A. Claye, J. E. Fischer, and A. Metrot, Chem. Phys. Lett. **330**, 61 (2000).
[22] J. Z. Bao, C. C. Davis, and R. E. Schmukler, IEEE Trans. Biomed. Eng. **40**, 364 (1993).
[23] R. Gómez *et al.*, Biomed. Microdevices **3**, 201 (2001).
[24] E. Katz and I. Willner, Electroanalysis **15**, 913 (2003).
[25] H. P. Schwan, in *Physical Techniques in Biological Research*, edited by W. L. Nastuk (Academic, New York, 1963), Vol. 6, pp. 323–406.
[26] H. Pauly and H. P. Schwan, Biophys. J. **6**, 621 (1966).
[27] R. A. Hoffman and W. B. Britt, J. Histochem. Cytochem. **27**, 234 (1978).
[28] H. Morgan, T. Sun, D. Holmes, S. Gawad, and N. G. Green, J. Phys. D **40**, 61 (2007).
[29] M. J. Hutchings and B. C. Blake-Coleman, Meas. Sci. Technol. **5**, 310 (1994).
[30] U. D. Larsen, G. Blankenstein, and S. Ostergaard, Proceedings of Transducers 1997, Chicago, USA, 1997 (unpublished).
[31] N. Xiang and K. Genuit, Characteristic Maximum-Length Sequences for the Interleaved Sampling Method, *ACUSTICA-acta acustica* Vol. 82 (1996), pp. 905–907.
[32] S. Gawad, L. Schild, and P. Renaud, Lab Chip **1**, 76 (2001).
[33] S. Gawad, K. Cheung, U. Seger, A. Bertsch, and P. Renaud, Lab Chip **4**, 241 (2004).
[34] D. Holmes, N. G. Green, and E. Morgan, IEEE Eng. Med. Biol. Mag. **22**, 85 (2003).
[35] K. Asami, T. Yonezawa, H. Wakamatsu, and N. Koyanagi, Bioelectrochem. Bioenerg. **40**, 141 (1996).
[36] K. Cheung, S. Gawad, and P. Renaud, Cytometry **65A**, 124 (2005).
[37] R. E. Scholfield, Electron Technol. **37**, 389 (1960).
[38] W. D. T. Davis, Control **10**, 302 (1966).
[39] N. Xiang, Signal Process. **28**, 139 (1992).
[40] B. Onaral and H. P. Schwan, Med. Biol. Eng. Comput. **21**, 210 (1983).
[41] H. A. Pohl, *Dielectrophoresis* (Cambridge University Press, Cambridge, UK, 1978).
[42] P. R. C. Gascoyne, X. B. Wang, Y. Huang, and F. F. Becker, IEEE Trans. Ind. Appl. **33**, 670 (1997).
[43] G. Fuhr, H. Glasser, T. Muller, and T. Schnelle, Biochim. Biophys. Acta **1201**, 353 (1994).
[44] J. Borish and J. B. Angell, J. Audio Eng. Soc. **31**, 478 (1983).
[45] D. V. Sarwate and M. B. Pursley, Proc. IEEE **68**, 593 (1980).
[46] F. J. Macwilliams and N. J. A. Sloane, Proc. IEEE **64**, 1715 (1976).
[47] M. Cohn and A. Lempel, IEEE Trans. Inf. Theory **23**, 135 (1977).
[48] N. Xiang and K. Genuit, Acustica **82**, 905 (1996).
[49] H. D. v. Lüke, Frequenz **40**, 215 (1986).
[50] M. Frigo, Proceedings of the ACM SIGPLAN Conference on Programming Language Design and Implementation (PLDI), Atlanta, Georgia, 1999 (www.fftw.org).